Soil Dynamics and Earthquake Engineering 127 (2019) 105855

Contents lists available at ScienceDirect

Soil Dynamics and Earthquake Engineering

journal homepage: www.elsevier.com/locate/soildyn

Comprehensive amplification estimation of the Indo Gangetic Basin deep soil sites in the seismically active area

Ketan Bajaj, P. Anbazhagan*

Indian Institute of Science, Bangalore, India

ARTICLE INFO

Keywords:
Deep basin
Seismic site classification
Amplification
Seismic site factors
Acceleration design response spectra
Site response study

ABSTRACT

Site amplification coefficients and acceleration design response spectra (ADRS) for the deep Indo-Gangetic Basin (IGB) have been proposed. Non-linear site response analysis is carried out at 275 deep shear wave velocity (V_S) profiles by selecting the input motion based on seismic hazard map for 10% probability of exceedence in 50 years. The spatial variation map of peak ground acceleration (PGA) and spectral acceleration (SA) at surface and various depths for the IGB are also presented. The bedrock PGA of 0.03–0.24 g increased to 0.1–0.97 g at surface and 0.05–0.35 g at a depth of 150 m. Maximum SA is observed between 0.08 s and 0.5 sec. The new site factors viz. F_a and F_v are derived for newly defined spectral period range. Further, ADRS is constructed which depends on PGA and seismic site class as per NEHRP. Proposed ADRS is compared with different deep basin studies and BIS:1893.

1. Introduction

The Indo-Gangetic Basin (IGB) is one of the world's largest regions of the Quaternary alluvial sedimentation having high spatial variable in the sedimentary thickness. Any earthquake in the contiguous Himalayan arc can produce seismically induced hazards (e.g. liquefaction, landslides or amplified ground shaking) in the deep IGB. Many authors [e.g. 1] have predicted the occurrence of the large earthquake in the Himalayan arc, the Indian Kashmir [e.g. 2], and the Himalayan segments in Sikkim, Bhutan and Arunachal [e.g. 3]. Ambraseys [4] reported that past earthquakes in the Himalayan region have caused extensive damage in the IGB. Medvedev–Sponheuer–Karnik (MSK) intensity maps developed by Hough and Bilham [1] depicted the 1–3 units' higher intensity in basin and 3 near to river banks and flood plains. Srinagesh et al. [5] concluded the amplification in peak ground acceleration (PGA) by a factor of 2–4 due to the presence of the softer material in the IGB. For predicting the future seismic hazard in the IGB, it is necessary to understand the amplification of seismic waves due to deep deposits in the basin.

Anbazhagan et al. [6] highlighted that the local site effect is the major factor that causes the damage due to an earthquake. 1985 Mexico (M_w 8.0), and 1989 Loma Prieta (M_w 8.0) are the two classical examples of earthquakes that illustrate the consequences of local site effect due to site amplification. 2001 Bhuj (M_w7.7), 1999 Chamoli (M_w 6.8), 2011 Sikkim (M_w 6.9), and 2015 Nepal (M_w7.8) earthquakes are the recent examples that explain the effects of soft and thick soil deposits on site-specific damage in the Indian subcontinent. These local site effects should be quantified properly for minimizing the earthquake induced effects that depend on the accuracy of the site response analysis. Many researchers [e.g. 7–13] estimated the site-specific local site effects considering both deep and shallow soil sites. Similarly, various researchers have studied the local site effects and estimated the amplification factors considering shallow sites for the Indian subcontinent [e.g. 14–19 etc.]. Most of these studies are either limited to soil column of 30 m depth or are provided with the layout for the site-specific analysis for the Indian subcontinent. Additionally, in many of these pervious works, V_s was determined from the measured SPT-N using empirical relationships and used for the site response studies. Moreover, in the previous site response studies, the input ground motions were either selected randomly from global database or simulated based on the occurred earthquake scenario. Till today there are no comprehensive studies available for estimating the local site effect for the deep deposits of IGB considering the measured V_s profiles for more than 100 m depth.

One of the aims of the study is to develop the shear wave velocity profile for deeper depth of the IGB. For this purpose, multichannel analysis of surface wave (MASW) survey has been done at 275 locations in Punjab, Haryana, Uttar Pradeshand and Bihar state in the IGB. These sites are classified and characterized based on time averaged V_s in the upper 30 m depth (V_{S30}) as per NEHRP [BSSC, 20] seismic site classification. Further, non-linear site response analysis has been carried out at these 275 locations. The input ground motions are selected based on seismic hazard map developed considering 10% probability of

* Corresponding author.
E-mail addresses: ketanbajaj@iisc.ac.in (K. Bajaj), anbazhagan@iisc.ac.in (P. Anbazhagan).

https://doi.org/10.1016/j.soildyn.2019.105855
Received 11 November 2018; Received in revised form 31 May 2019; Accepted 4 September 2019

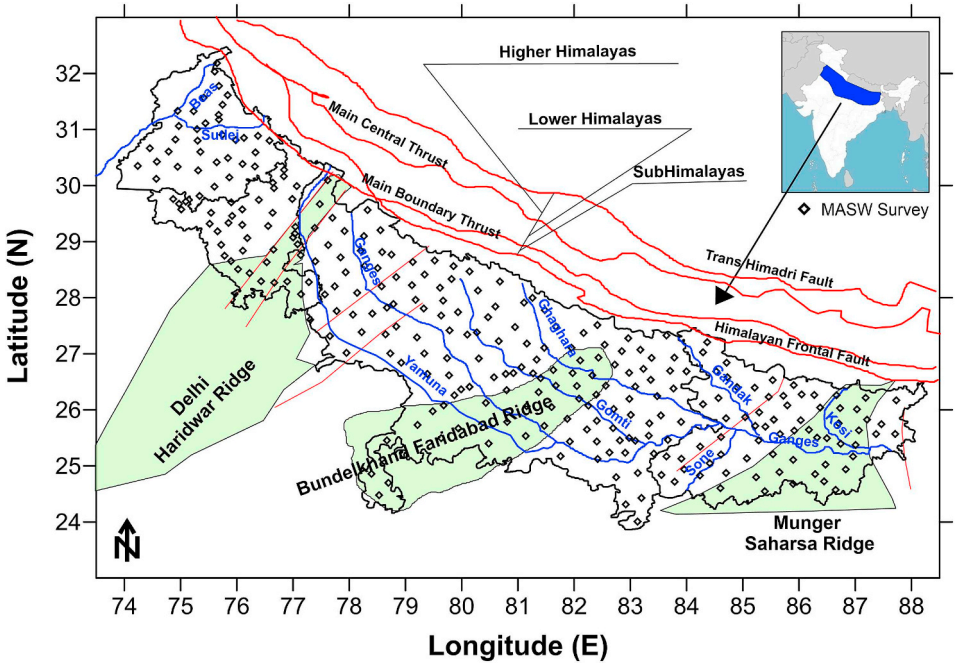

Fig. 1. Different tectonic features and MASW survey locations in a study area.

exceedence in 50 years value at bedrock. Both the locally recorded and simulated ground motions have been used for site response study. The site factors at short period or 0.2 s (F_a) and long period or 1.0 s (F_v) defined by the American Society of Civil Engineer's Standard ASCE 7–10 (ASCE) [21], the International Building Code (ICC) [22], and the AASHTO guide [23]. Site factors at zero period (F_{PGA}), F_a and F_v have been calculated by newly derived spectral period based on the surface response spectra. These site factors are further used in deriving the acceleration design response spectra (ADRS) for the deep basin in the IGB for different site classes and PGA values. The compatibility of the new ADRS has been compared with the NEHRP and other studies.

2. Study area

The IGB is well known as the Himalayan foredeep depression, and it is situated between the Indian Peninsular Shield and the Himalaya region. It is formed due to post-collision between the Indian and the Asian tectonic plates during the Cenozoic growth of the Himalayas. IGB inhabits an area around 2,50,000 km^2 and lies roughly between longitude 74° E and 88° E, and latitude 24° N and 32° N (See Fig. 1). The sediment structure and thickness of the IGB was studied using geophysical study and deep drilling [24–26] and joint inversion of receiver function [e.g. 27]. The sediment thickness in the IGB is asymmetric and varies from few tens of meters in the south and progressively increases the thickness up to ~5–6 kms in the northernmost part. Addition to variable thickness, the IGB consists of number of ridges and depressions (Fig. 1). The detail descriptions about these ridges can be referred from Singh [28].

Including the Himalayan, the Ganga Plain foreland basin is also experiencing the strong compressional stress conditions. Hence the IGB exhibits some tectonically-controlled geomorphic features which are formed under stress conditions, and some older tectonic features are reactivated and have become active lineaments [28]. Several researchers [e.g., 24, 26, 28 etc.] have acknowledged the tectonic framework of the Indo-Gangetic Basin. The high neotectonic activity in the IGB is reported by various researchers [e.g. 29, 30 etc.] considering the skewness of fan surface, a sudden change in the direction of alignment of the river, displacement of Siwalik hills, etc. Few classical examples of earthquakes that shows the site amplification in the basin are 1934 Nepal/Bihar (M_w 8.2), 1905 Kangra (M_w 7.9), 1999 Chamoli (M_w 6.8) and 2015 Nepal (M_w 7.8) earthquakes. 1999 Chamoli (M_w 6.8) earthquake caused ground shaking in the northern part of Haryana and eastern part of Uttar Pradesh and Bihar [31]. 1934 Nepal/Bihar (M_w 8.2) earthquake caused extensive damage in the Ganga plain and Bihar province of India for half a century following the shock.

3. V_S Variation in the IGB

Multichannel analysis of surface wave (MASW) is a widely used geophysical survey for evaluating the ground stiffness by measuring the shear wave velocity of the subsurface. In the present study, 24 channels Geode seismograph in combination with 24 vertical geophones with the frequency of 2.0 Hz has been used for determining the V_s profile in the IGB. For acquiring the raw data, both passive and active MASW has been done at the sites, as given in Fig. 1. The active data has been recorded by striking a 12 kg sludge hammer against a 30 cm × 30 cm for generating the surface waves. For recording the data in passive MASW survey, passive roadside acquisition method has been used. The spacing between the geophones varied from 1 to 3 m in case of active survey and 1–5 m in case of passive survey. At each survey location, minimum of 5 multiple shots are stacked to increase the signal to noise ratio (SNR). For acquiring the raw data considering the passive survey, different sampling intervals (2 m s–8 m s) and recording times (30 sec–120 sec) are used to enhance the dispersion curve quality. Further the acquired data using both active and passive MASW surveys, the individual dispersion curves have been extracted from velocity–frequency images. Two seventy five MASW surveys were carried out in the entire stretch of IGB and is shown as Fig. 1.

The V_s profiles of each location were determined using window-based program named 'SurfSeis 5' and 'ParkSEIS 2'. Details regarding the processing of data can be found in Park et al. [32,33] and Xia et al. [34]. At each location, dispersion curve (DC) was extracted for 5–50 Hz in case of active and 2–20 Hz in case of passive MASW survey. For inverting the DC, 15 to 18 layered earth model [33] is considered at initial stage of inversion. Using the optimization technique [34], 1D shear wave velocity was calculated for each iteration. Root mean square (RMS) is considered as an indicator for the closeness between theoretical and observed DC. The detail description about the data acquisition and processing are given in Bajaj and Anbazhagan [35].

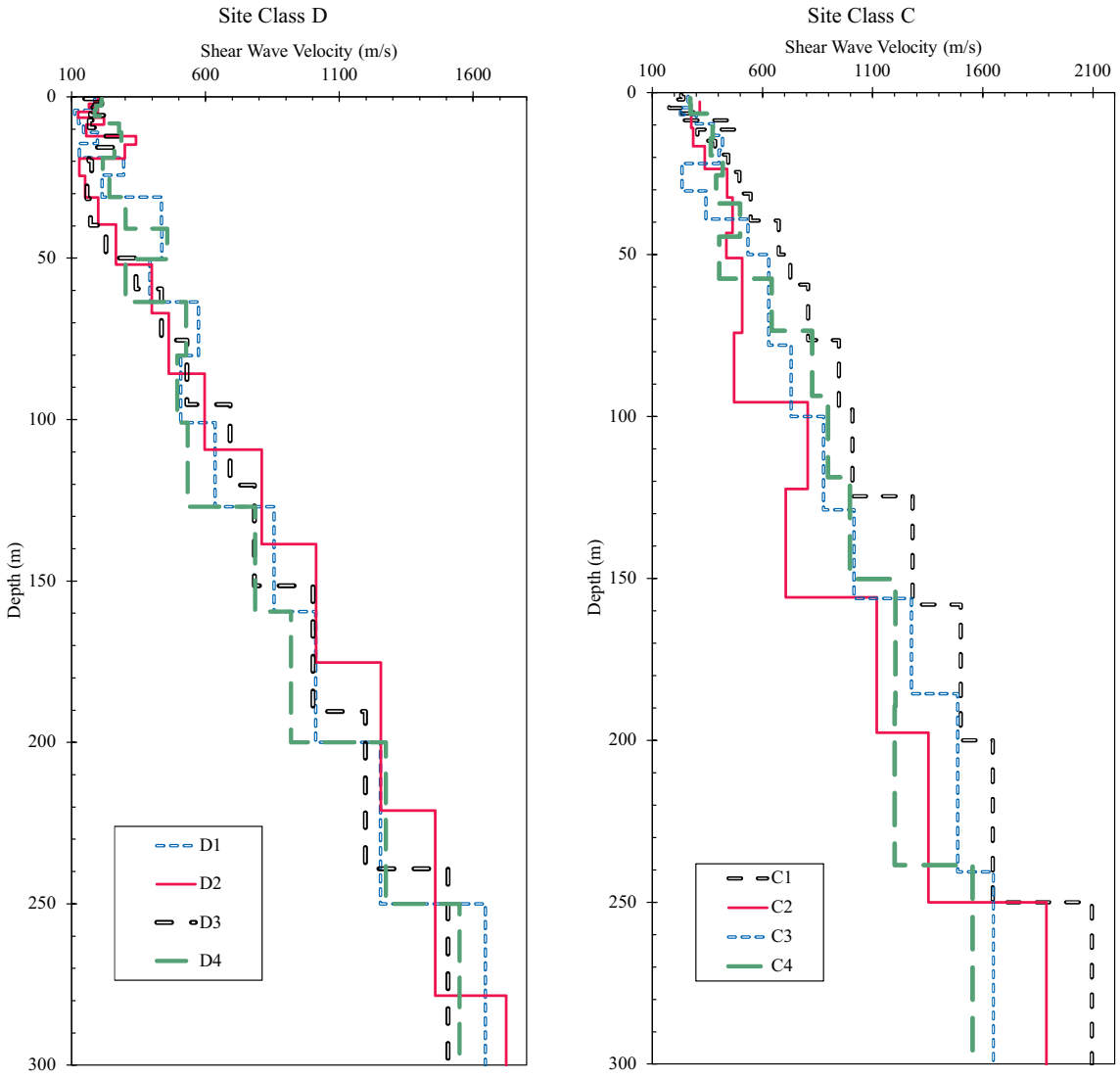

Fig. 2. Typical variation of shear wave velocity with depth for NEHRP seismic site class C and D.

For the first 10 m the average V_S varies from 150 to 800 m/s and it increased to 160–1206 m/s at a depth of 30 m. Out of 275 profiles, more than 50% of the profiles have V_{S30} in between 183 and 357 m/s. The V_S at 150 m depth varies from 1050 to 1890 m/s. The typical variation of V_S with depth for seismic site class C and D as per NEHRP is given as Fig. 2. The variation of shear wave velocity of entire IGB can be found in Bajaj and Anbazhagan [35].

4. Input soil properties

Shear modulus degradation (G/G_{max}) and hysteric damping ratio curves versus shear strain are the salient properties in any site response studies. In deep deposits, such as IGB, overburden pressure plays a vital role in determining the dynamic properties of soil. However, in general soil displays stiffer characteristics with depth [36]. In literature various pressure dependent G/G_{max} and damping ratio are available for different types of soil. Depending on the type of soil, different researchers have used different curves for deep and shallow deposits. For e.g. Malekmohammadi and Pezeshk [36] used EPRI [37] for deep Mississippi Embayment. However, Aobey et al. [13] used Zhang et al. [38] curve for deep deposits in Charleston, South Carolina. Considering the KiK-net data, Anbazhagan et al. [39] suggested different curves for different soil deposits. Bajaj and Anbazhagan [40] further modified the conclusions by using wide range of G/G_{max} and damping ratios for both shallow and deep profiles of KiK-net downhole array. Based on the analysis on residuals, Bajaj and Anbazhagan [40] suggested EPRI [37], Menq [41], Zhang et al. [38] and Darendelli [42] about G/G_{max} and damping ratios for rock, gravel, sand and clay predominate profiles respectively.

For most of the lithology logs available for Punjab and Haryana region, clay/silt is predominant for first 30 m, and sandy gravel soil is mostly available after 60 m depth. Clay available in Punjab Haryana region is having high plasticity and is mixed either with kankar or gravels. Uttar Pradesh is mostly dominated by silty clay and medium sand at different depths. For many places, alternative layers of clay and sand with kankar or gravel are available. First 50 m of Bihar is dominated by silt and clay. From 50 to 150 m, alternative layers of clay and medium or coarse sand are available. Studying all these details nearby MASW sites, shear velocity layers have been broadly classified as rock, gravel, sand and clay. Hence, considering Bajaj and Anbazhagan [40] study of EPRI [37], Menq [41], Zhang et al. [38] and Darendelli [42], G/G_{max} and damping ratio has been used for the rock, gravel, sand and clay predominate profiles respectively. These curves are given as Fig. 3. For some of the profiles, soil properties after 150 m depth could not be determined, depending on the overburden pressure and geological units, either EPRI [37] or Zhang et al. [38] curves have been used. Sites where plasticity index (PI) are not available, general PI value of 0, 15 to 20 and 30–60 has been considered respectively for sand, silt and clay

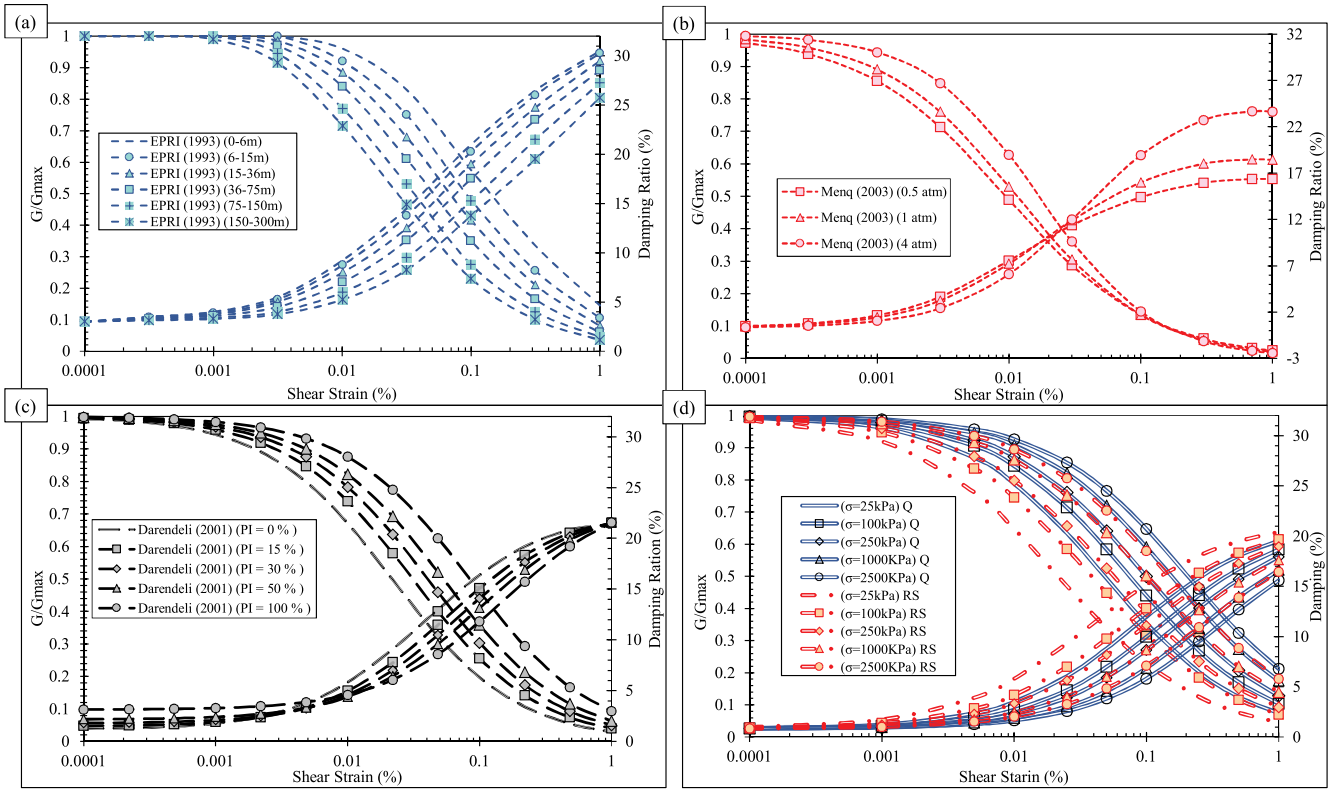

Fig. 3. Depth dependent shear modulus degradation (G/G_{max}) and hysteric damping ratio curves as proposed by (a) EPRI (1993), (b) Menq (2003), (c) Darendeli (2001), and (d) Zhang et al. (2005) used in site response analysis.

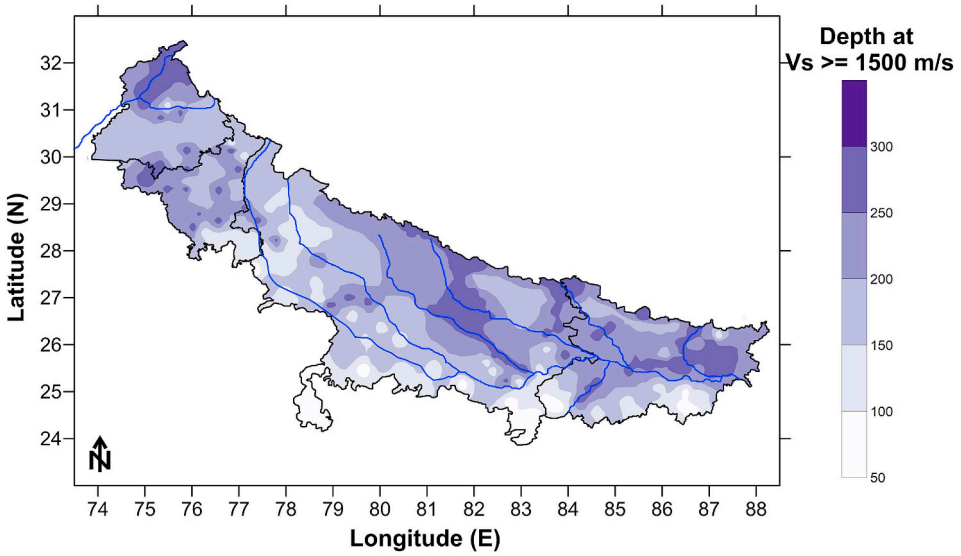

Fig. 4. Spatial variation of depth at which shear wave velocity is more than 1500 m/s.

[40,43]. For Zhang et al. [38], geological units are taken from GSI geological quadrangle maps. Further, in-situ density of each layer is estimated using relationship developed by Anbazhagan et al. [44]. The correlation used is

$$\rho = 0.52V_S^{0.2} \quad (1)$$

Here, ρ is the density in g/cc and V_s is in m/s.

The coefficient of lateral earth pressure at rest (K_o) is computed using theoretical relationship between K_o and Poisson's ratio (ν) i.e.

$$K_o = \nu/(1-\nu) \quad (2)$$

where. $\nu = (V_p^2 - 2V_S^2)/(2V_p^2 - 2V_S^2)$

The depth of ground water table has been taken from the ground water year book 2016–2017 published by Central Water Board of India in 2017 (http://cgwb.gov.in/Ground-Water/Groundwater%20Year%20Book%202016-17.pdf, last accessed July 2018). It can be noted here that, in the absence of any other source of information, it has been considered that these subsoil properties are not differing much between the MASW test location and the nearby borehole.

Site amplification is also affected by the depth of bedrock and velocity of the reference rock. Barani et al. [45] concluded that soil thickness plays a vital role on those places where bedrock depth is

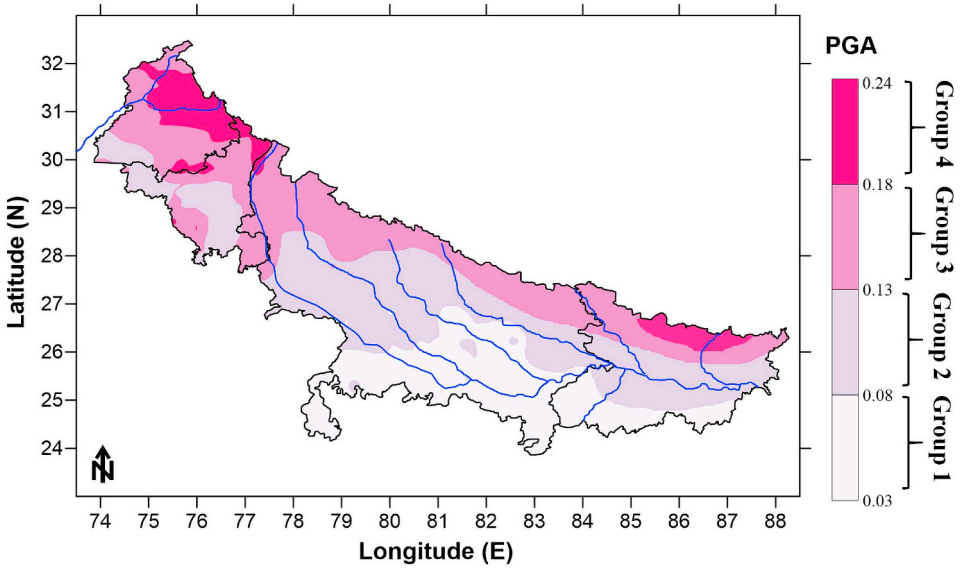

Fig. 5. Spatial variation of peak ground acceleration (PGA) value at bedrock by diving it into four regions.

unknown or largely uncertain. Malekmohammadi and Pezeshk [36], studied the effect of bedrock depth on amplification for deep Mississippi Embayment. The reference rock velocity in this study is considered as 3000 m/s following the recommendation of the Geotechnical Working Group of the Next Generation Attenuation-East [46]. However, Silva et al. [47] and Kwok and Stewart [48], determined the amplification factor by considering the bedrock reference velocity as 1000 m/s. Aobey et al. [13] determined the amplification factor considering half space velocity as 700 m/s after 137 m depth for Charleston, South Carolina. For Indian subcontinent, most of the studies [e.g. 18, 49] determined the amplification factor by considering the bedrock velocity more than 760 m/s or V_s of the bottommost layer. Anbazhagan et al. [50] has observed no significant difference in response spectra at surface when ground motion is inputted at bedrock having V_s between 1385 and 1868 m/s for shallow sites. Ghofrani et al. [51] suggested that the amplification of the data in the range of 760–1500 m/s appeared to be similar to the depth of installation where Vs is more than 1500 m/s. However, in most part of the IGB, the bedrock depth is not identified in detail. Hence to estimate the reliable amplification factor for IGB, input motion is given at the layer having velocity 1500 m/s. The spatial variation of depth having $V_s \geq 1500$ in the entire IGB is given as Fig. 4.

5. Input ground motion and site response analysis

Bed-rock motion is the pre-requisite for any site response study. In the absence of recorded ground motion, 1940 El-Centro, 1985 Mexico, 1989 Loma Prieta, 1994 Northridge, 1995 Hyogoken-Nanbu and 1999 Chi-Chi etc. had been widely used for many site response studies in the Indian subcontinent. These motions were either used directly or scaled up to the required PGA for a site. Because of lack of recorded ground motions, stochastically simulated ground motions are widely used in many site response studies. Various authors [e.g. 52–54 etc.] generated the synthetic ground motions consistent with uniform hazard spectra and hazard values of a study area for site response studies. Ansal and Tonuk [55] concluded that irrespective of method followed for seismic hazard analysis, both the simulated and recorded ground motions can be used for site-specific response studies. The characteristics of input base or bedrock motion which controls the response of any soil column are the frequency content, amplitude and duration. These three characteristics control the local soil condition during an earthquake. Considering the recorded ground motion which were recorded elsewhere may not give the reliable estimate of site amplification. Moreover, selecting one ground motion by acknowledging only amplitude from seismic hazard analysis or seismic hazard deaggregation may not reflect the base motion completely regarding the frequency content duration.

A wide range of recorded motions are available for the Himalayan region, which was collected by Anbazhagan et al. [56] and characterized station sites based on the recorded earthquake data. The ground motions recorded at rock sites [56] are used for the site response analysis of the IGB. The seismic hazard map for 10% probability in 50 years at bedrock level for the IGB has been used as the preliminary criteria for ground motion selection. The return period for 10% probability in 50 years is referred as design-based earthquake in Bureau of Indian Standard (BIS:1893) [57]. The seismic hazard map of IGB is given as Fig. 5. The details regarding the PSHA can be referred from Bajaj and Anbazhagan [58]. The bedrock PGA varies from 0.03 to 0.24 g (Fig. 5). The entire PGA variation has been divided into four bins as (a) 0.03–0.08 g, (b) 0.08–0.13 g, (c) 0.13–0.18 g, and (d) 0.18–0.24 g. These are further referred as group 1 (G1), group 2 (G2), group 3 (G3) and group 4 (G4) respectively. Fifty ground-motions that have occurred in the Himalayan region and recorded at bedrock sites (Anbazhagan et al., 56) have been studied preliminarily. The significant duration for these four groups varied as (a) 8.23–52.5 sec; (b) 11.53–35.22 sec; (c) 11.22–30.25 sec; and (d) 9.23–25.25 sec based on the recording. However, the frequency of the motion varies from 3.25 Hz to 10 Hz in all the four groups. Typical shear wave velocity profiles for site class C and D for all the four groups is given as Fig. 2. These recorded motions have moment magnitude (M_w) between 5.2 and 7.8 and a hypocentral distance (R) between 17 and 400 km with PGA varying from 0.023 to 0.27 g. As the recorded earthquake motions could not cover the entire range of magnitude, hypocentral distance and bedrock PGA for the IGB, hence, the stochastically simulated ground motions are also used. The synthetic ground motion data is generated using the Finite-Fault stochastic model (EXSIM) developed by Motazedian and Atkinson [59] and improved by Boore [60].

For determining the site amplification in each site, 10 ground motions have been used depending on variation of PGA, frequency and duration of ground motion. For example a site X's calculated PGA for 10% probability in 50 years is 0.12 g, it lies in group 2 (i.e. PGA between 0.08 and 0.13 g). Firstly, for this site, recorded ground motions are selected between 0.11 and 0.13 g. If 10 recorded ground motions are not available between 0.11 and 0.13 g with different frequency and duration, in that case synthetic ground motion has been used. Typical bedrock motion of D4 site (see Fig. 2) is given as Fig. 6. The determined bedrock PGA for D4 is 0.235 g, based on the bedrock PGA, 10 ground motions have been selected between 0.22 and 0.26 g. However, only

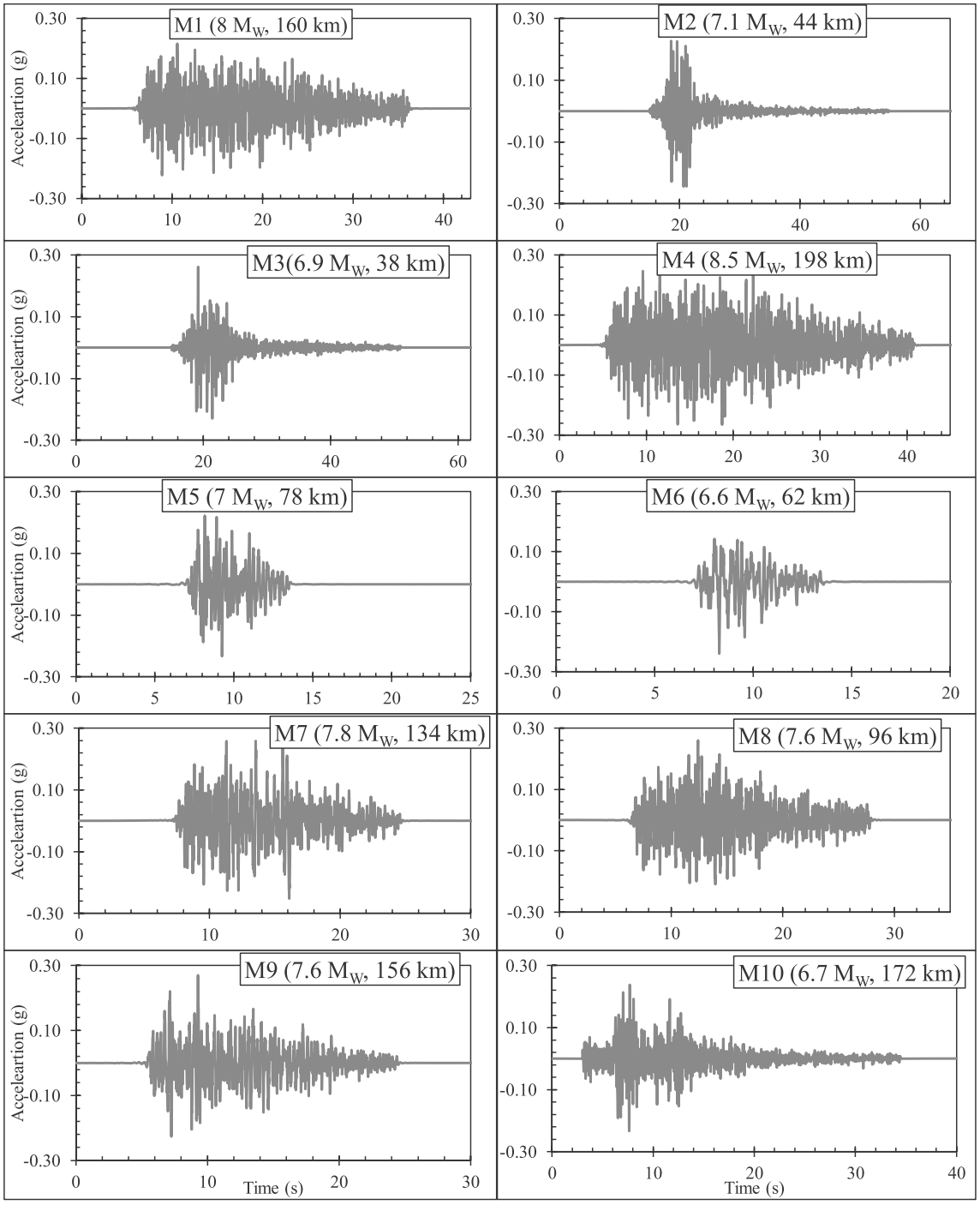

Fig. 6. Typical plot of bedrock acceleration time history used in site response analysis of D4 site.

four recorded ground motions are available in this range of PGA, hence, in this case six ground motions have been simulated for different durations and frequencies (see Fig. 6).

Various software (SHAKE91, DEEPSOIL, STRATA etc.) are available for performing 1 dimensional (1D) total stress ground response analysis. In this study, DEEPSOIL has been used to perform both the non-linear and equivalent linear 1D total site response analysis for determination of amplification factors for IGB. DEEPSOIL was developed to understand the nonlinear behavior of the deep Mississippi basin [61]. Hence, DEEPSOIL provides an option for extended Rayleigh damping which is more appropriate for deep profiles [12]. The details regarding the DEEPSOIL can be found in Hashash et al. [62]. The thicker layers should be subdivided in such a way that a minimum fundamental frequency should be between 15 Hz and 25 Hz because higher frequencies contain a relatively small amount of energy in an earthquake loading [63]. Site effect is generally divided into three parts: soil column response, basin effects, and topographic effects. It is important to note here that, alike Malekmohammadi and Pezeshk [36], basin and topographic effects are considered small in the IGB and are not addressed in this study.

6. Analysis and results

For performing the non-linear site response analysis, DEEPSOIL [62] has been used. The V_s for each layer and corresponding soil type, depth of water table and unit weight of soil at corresponding depths have been provided as input parameters in DEEPSOIL. This information has been

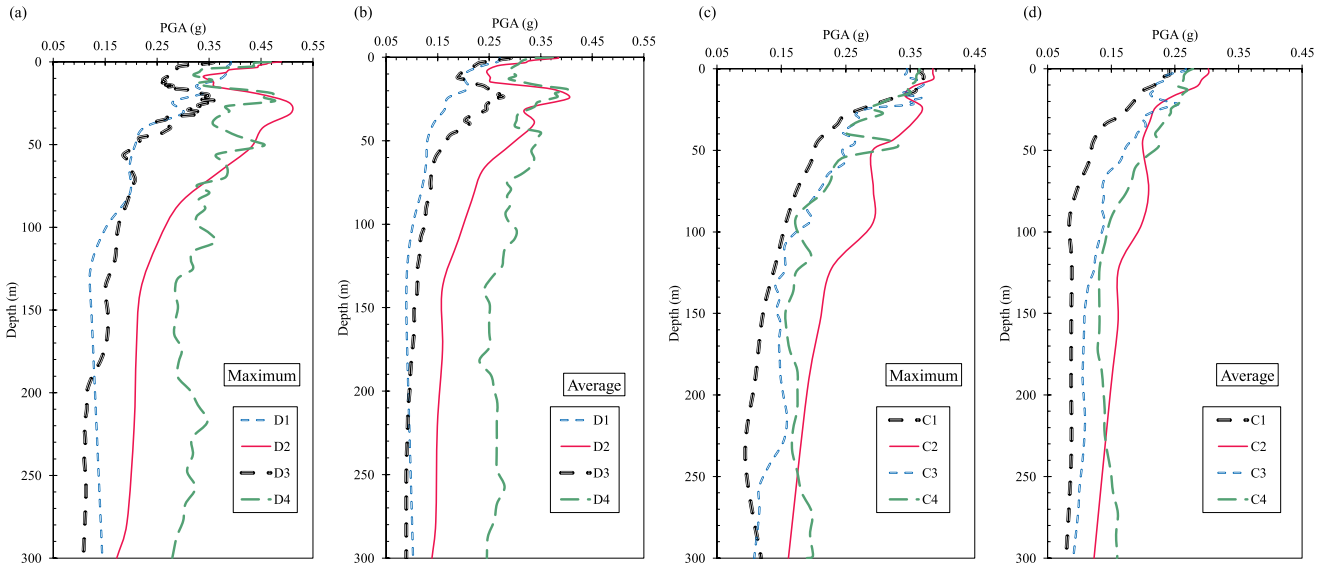

Fig. 7. Typical variation of maximum and average PGA with depth for the shear wave velocity profiles given in Fig. 2.

collected from various sources as explained above. At each site, 10 selected motions are assigned as base motion in each site. Hence in total 275 × 10 = 2750 nonlinear analysis have been performed to understand the site response characteristics of the IGB. For all the analysis, the motion is applied for time domain with an elastic base. Typical variation of PGA for the sites presented in Fig. 2 is given as Fig. 7. It can be seen from Fig. 7 that variation in PGA value from 200 to 300 m is not significant in all the cases. However, beyond 100 m, there is a sudden change in PGA values with depth as it reaches to surface. At D2 and C4, the maximum PGA at bedrock is 0.17 g and 0.18 g, however the surface PGA is observed as 0.49 g and 0.36 g respectively. Similarly, for D1, D2, D3 and D4, the average PGA at bedrock is 0.102, 0.148, 0.079, 0.235 g and the average PGA at surface is observed as 0.312 g, 0.384 g, 0.293 g, 0.373 g respectively. Similar observations are made for other soil profiles and maximum and average PGA at surface and different depths are determined. The results are further used for determining the surface amplification factor.

Spectral parameters at surface and at different depths have been estimated. Typical variation of spectral acceleration at different depths of D2 site (see Fig. 2) is given as Fig. 8. It has been observed from Fig. 8 that spectral acceleration (SA) at different depths is different at different periods. A sudden increase in SA value has been observed at 32 m depth due to the presence of soft layer and significant decrease at a depth of 15 m. Moreover, at 32 m depth, SA is observed at longer period which is significantly decreased at the surface. Similar observations have been seen in various profiles in the IGB due to the presence of low velocity region at different depths. The detailed explanation of variation of PGA and SA value at different depths is given in next section. The results in the form of contour maps and graphs have been presented. Surface amplification time history and response spectra at the surface has been obtained at each site. Each site has 10 PGA and SA values from 10 ground motions. These are used to estimate the average and maximum PGA and SA for each site. The variation of maximum and average surface PGA and SA at 0.25 and 1.0 s for all the four groups is given as Table 1. Similarly, the duration of motion for all the four groups has been changed to (a) 15.23–73.5 sec; (b) 18.53–45.22 sec; (c) 17.22–45.25 sec; and (d) 15.23–31.25 sec. From Table 1, it can be concluded that bedrock motion amplifies with increase in the duration and the amplitude of the input motion.

6.1. Spatial variation of spectral parameters at surface

The spatial variation of maximum and average PGA at surface is given as Fig. 9. The average and maximum surface PGA varies from 0.1 to 0.75 g and 0.1–0.97 g respectively. The maximum surface PGA varies from 0.09 to 0.52 g, 0.15–0.73 g, 0.17 to 0.68 g, and 0.35–0.93 g for group 1, group 2, group 3 and group 4 respectively. For more than 70% of the IGB area, the maximum and average surface PGA respectively is in the range of 0.35–0.50, and 0.2–0.35 g for 10% probability in 50 years. Most of the area near to the river varies from 0.20 to 0.50 g (Fig. 9a). The maximum surface PGA of 0.5–0.97 g has been observed in the northern part of Punjab and Haryana.

Further, the maximum and average surface spectra are obtained from the 10 ground motions. The variation of maximum bedrock spectra with surface spectra for all the four groups is given as Fig. 10. The average SA at different periods i.e. 0.02, 0.05, 0.2, and 1.0 s at surface have been obtained from site response spectra and plotted as Fig. 11. The average SA for most of the IGB at zero period increased from 0.20 to 0.35 to 1.00–1.85 g at 0.2 sec and changes to 0.40–0.60 g at 1 sec. For most of the sites the maximum spectral acceleration has been observed between 0.08 sec and 0.5 sec in the IGB. Further the SA is divided by the rock spectral acceleration and ratio has been obtained. Based on the observation, it can be determined that peak SA varies from 3.50 to 10.20 g. The maximum ratio has been observed between 0.2 and 0.4 sec. The maximum SA is observed between 0.2 and 0.4 sec in Punjab and Haryana region and few parts of Uttar Pradesh and Bihar near to the rivers. The SA value varies from 0.78 to 1.65 g in these regions. The average SA in Uttar Pradesh region at zero period was 0.22–0.35 g, which has been increased to 0.79–1.62 g. Similarly, for Bihar, SA increased from 0.1 to 0.4 g at zero period to 0.38–1.76 g at spectral period between 0.2 and 0.43 sec. The maximum SA value of 1.96 g has been observed at 0.3 sec near to the northern part of the Punjab and Haryana region. For group 1 and 2, the maximum spectral acceleration has occurred at spectral period between 0.08 and 0.2 sec. However, for group 3 and 4, maximum SA has occurred between 0.15 and 0.5 sec. The high value of PGA and SA is observed near to the northern end and central part of Uttar Pradesh and Bihar region. This may be due to the presence of loose deposits at the surface near to the river bed.

Further, the distribution of PGA has been studied at different depths for the same input motion. This is because of the significant variation of shear wave velocity at different depths in IGB. The spatial variation of max PGA at 10, 30, 50, 100 and 150 m has been plotted and given as Fig. 12. The distribution of maximum PGA at a surface decreases from 0.1 to 0.97 g to 0.05–0.35 g at a depth of 150 m. However, the significant variation in PGA is not observed in the northeastern part of Punjab and Haryana till 100 m. Similarly, near to the Kosi river and in the north side of Ganga river in Bihar, PGA does not vary significantly with depths. The PGA value decreases with the depth at central part of Uttar Pradesh. This may be due to the presence of the ridges in the central part of the Uttar Pradesh.

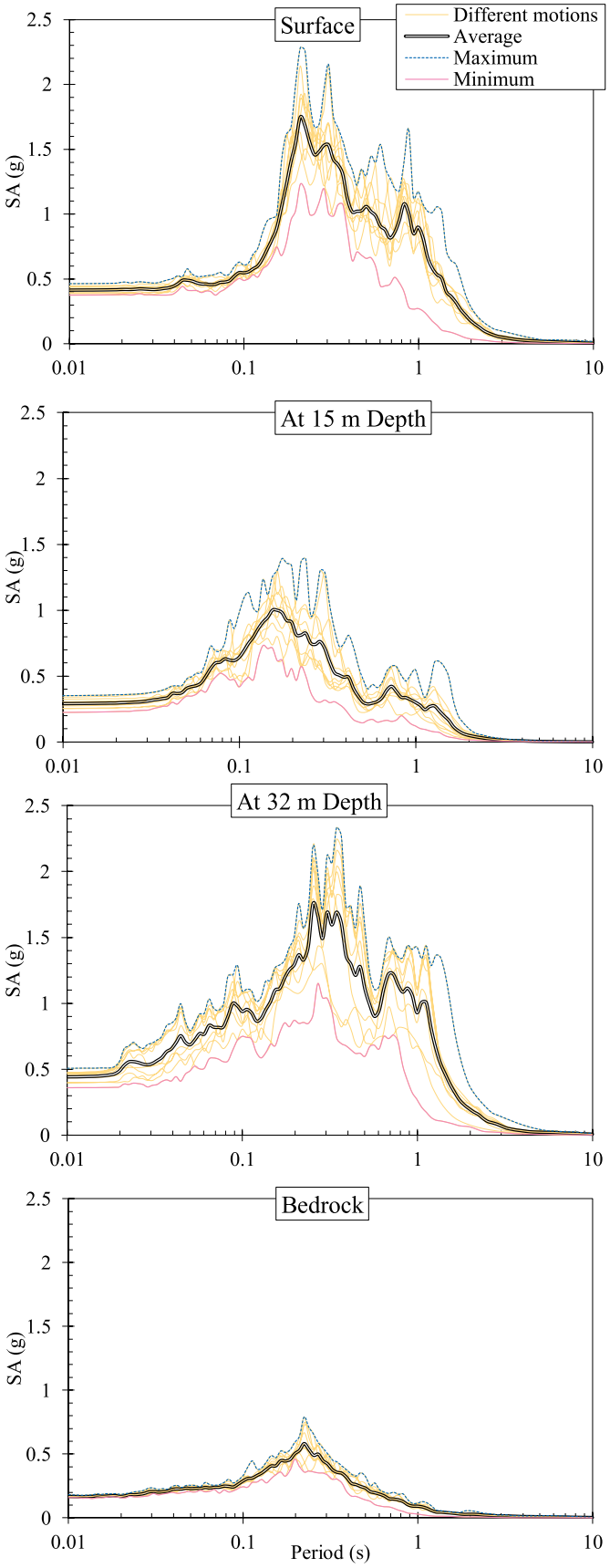

Fig. 8. Variation of spectral acceleration (SA) at different depths.

In the Punjab-Haryana region, PGA at surface, 30 m and 100 m depth respectively varies from 0.38 to 0.97 g, 0.32–0.79 g and 0.25–0.58 g. The high PGA is observed near to the Satluj and the Beas rivers, this is due to the presence of loose sand deposits till 50–100 m depth with average velocity varying from 200 to 531 m/s. Near to the Yamuna river (the northernmost part of Haryana), higher value of PGA at 10 m is noted as compared to surface, which may be due to the presence of low velocity region because of loose soil deposits at shallow depths. The PGA and SA near to the northeast part of Punjab is low at 150 m as compared to another part, which may be due to the presence of granite or angular quartzite after 250 m depth (GSI, 2012). The UPR is mostly dominated by clay and sand at different depths. As per the geological quadrangle available for different places, UPR is covered with alternative layers of clay and sand with kankar or gravel (https://www.gsi.gov.in/). The PGA at surface and at 50 and 150 m depth respectively varies from 0.15 to 0.77, 0.08–0.31 and 0.061–0.23 g respectively. The PGA at bedrock, surface and at 50 m depth varies from 0.13 to 0.14g, 0.34–0.48g and 0.22–0.32 g respectively near to the upper Ganga plain. High PGA is observed at 10 m depth near to the Ganga-Yamuna interfluve, which may be due to weak silty clay deposits in this region. Similarly, due to the presence of alternative loose clayey deposits and shallow water table, high PGA and SA till 15 m depth is noted in the central part of Uttar Pradesh Region. The maximum surface SA occurs at spectral period between 0.25 and 0.38 sec in this region and it is decreased to 0.12–0.15 s at depth of 150 m. This may be due to the presence of the thick deposits of Varanasi older alluvium, as indicated by the GSI Lucknow quadrangle. The shear velocity at the middle Ganga region is low at shallow depths and increases significantly after a depth of 80 m. This may be the reason for sudden decrease in PGA value and spectral period at a depth of 100 m. The low amplification in PGA value at surface is observed in the southern part of Uttar Pradesh region which is due to the presence of high velocity region because of compacted quartzitic sandstone occurrence (Varanasi quadrangle, GSI). The high spatial variability of PGA and SA are observed in Bihar region. The top 50 m near to Sone megafan in Bihar is occupied by low velocity clayey muddy deposits, this is the reason of occurrence of high PGA of 0.45–0.62 g. However, PGA and SA decrease significantly after 50 m because of presence of high velocity dark grey, hard clay in the alternative ?? alternating with grey silt and fine sand (Muzaffarpur quadrangle, GSI). Due to the presence of low velocity region at top 10–80 m near to the Kosi and Gandak basin, high PGA at 10–30 m depth and SA is observed in this region. The upper 50 m near to Sone megafan in Bihar region is occupied by clay/muddy deposits underlined by brownish yellow fine to coarse sand interleaved with gravel layers (Muzaffarpur quadrangle, GSI). V_s of clay/silt in this region is 250 ± 30 m/s up to 50 m depth, hence high PGA and SA is observed at different depths as compared to surface. The PGA and SA are significantly less in the southern part of Bihar, because this area is covered with isolated ridges and mounds, and hills and highlands of the Chotanagpur Plateau (Gaya quadrangle, GSI). Due to the significant spatial variation of lithology and shear wave velocity, the considerable variation in PGA and SA at different depths and at surface are observed.

6.2. Amplification factors determination

The amplification factor is defined as the ratio of the intensity measurement of the motion at the soil surface to the corresponding value at the bedrock. The amplification at each period is defined as

$$\mathrm{Amp(T)} = \frac{\mathrm{SA_{Soil}(T)}}{\mathrm{SA_{Rock}(T)}} \tag{3}$$

where, $\mathrm{SA_{Soil}(T)}$ and $\mathrm{SA_{Rock}(T)}$ is defined as spectral acceleration of the motion at soil surface and bedrock respectively for the same period (T). Based on the observation in Fig. 7 (a) and (b), it is seen that amplification of 1.12–1.65 is observed from 200 to 300 m. However, beyond 100 m, it changes to 2.32 to 3.26 with depth as it reaches to surface. Similarly, study has been carried out for all the 275 profiles and

Table 1
Comparison of variation of bedrock PGA and SA at 0.25 and 1.0 s with the surface PGA and SA at 0.25 and 1.0 s

Description	Peak and Spectral Accelerations (g)			
Group (Refer Fig. 5)	I	II	III	IV
Maximum Surface PGA	0.030–0.080 g	0.080–0.130 g	0.130–0.180 g	0.180–0.240 g
Average Surface PGA	0.095–0.522 g	0.152–0.734 g	0.173–0.684 g	0.348–0.931 g
Average Bed-Rock SA (0.25 s)	0.063–0.423 g	0.096–0.558 g	0.132–0.521 g	0.307–0.817 g
Maximum Surface SA (0.25 s)	0.108–0.191 g	0.167–0.412 g	0.354–0.581 g	0.524–1.018 g
Average Surface SA (0.25 s)	0.185–1.742 g	0.182–3.696 g	0.503–3.154 g	1.087–4.761 g
Average Bed-Rock SA (1.0 s)	0.141–1.249 g	0.108–2.028 g	0.376–2.064 g	0.925–2.065 g
Maximum Surface SA (1.0 s)	0.029–0.076 g	0.041–0.085 g	0.047–0.107 g	0.122–0.182 g
Average Surface SA (1.0 s)	0.148–2.212 g	0.252–1.221 g	0.247–1.295 g	0.576–1.582 g
Maximum Surface PGA	0.074–0.541 g	0.141–0.808 g	0.164–0.851 g	0.324–0.872 g

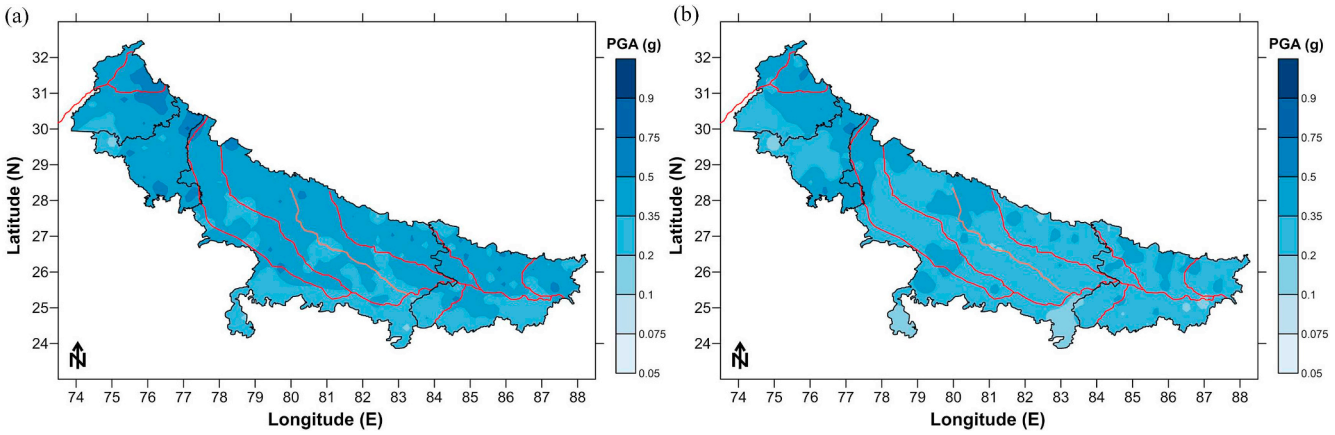

Fig. 9. Spatial variation of (a) maximum and (b) average surface peak ground acceleration (PGA) for the Indo Gangetic Basin.

distribution of implication has been plotted. The spatial variation of amplification factor is plotted as Fig. 13. The amplification factor at the surface varies from 1.32 to 6.28. For more than 90% of the area, the amplification factor is between 2.12 and 3.88. The considerable increase in amplification factor has been observed in the Bihar region. This is due to the presence of the low velocity clay and loose deposits near to Kosi, Sone and Gandhak river in the top 30–50 m. The amplification factor in Punjab-Haryana, Uttar Pradesh and Bihar region varies from 2.8 to 3.9, 1.5 to 3.4, 1.8 to 6.3 respectively.

Several authors have calculated amplification factor for various part of Indian subcontinent. Based on the microtremor studies, Sharma et al. [64] presented the amplification factor in the range of 2–3 for Delhi city. Based on equivalent linear approach, Anbazhagan et al. [6] and Kumar et al. [18] determined the amplification factor of 1.06–2.05 and 2.5 to 3.5 respectively for Lucknow urban center. Anbazhagan and Sitharam [16] and Boominathan et al. [15] calculated the amplification factor as 2 to 4 and 4.5 to 5.5 for Bangalore and Chennai respectively considering 30 m V_S profiles. Based on Horizontal to vertical spectral ratio, Kamal and Mundepi [14] determined amplification factor of 2–3 for Dehradun city. Govindraju and Bhattacharya [49] determined amplification factor of 4.4–4.8 for Kolkata city by using equivalent linear approach. Phanikanth et al. [65] and Naik and Choudhury [17] determined the amplification factor of 2.37–3.44 and 2.96 respectively for Mumbai and Goa. Similarly, Kumar et al. [19] derived the amplification factor in the range of 1.0–7.4 for Delhi city using equivalent linear approach and V_S up to 30 m depth. In this study, the amplification factor varies from 1.32 to 6.28 while inputting motion at V_s more than 1500 m/s, which is comparable with the amplification factor determined by Sharma et al. [64] using microtremor.

7. Determination of site coefficient for IGB

The site coefficients at short period or 0.2 s (F_a) and long period or 1.0 s (F_v) have been adopted by ASCE [21], ICC [22] and AASTHO [23]. F_a and F_v were defined in Borcherdt [66] as

$$F_a = \frac{R_{Soil}}{R_{Rock}} \frac{1}{0.4} \int_{0.1}^{0.5} \frac{RS_{Soil}(T)}{RS_{Rock}(T)} dt \quad (4)$$

$$F_v = \frac{R_{Soil}}{R_{Rock}} \frac{1}{1.6} \int_{0.4}^{2.0} \frac{RS_{Soil}(T)}{RS_{Rock}(T)} dt \quad (5)$$

where, RS_{Soil} and RS_{Rock} are response spectra at soil and rock at given spectral period T respectively. R_{Soil} and R_{Rock} respectively are the hypocentral distance at soil and rock stations. As in the present study $\frac{R_{Soil}}{R_{Rock}}$ is assumed to be 1.0 as the hypocentral distance for rock and soil station is similar. These site coefficients are determined using spectral period ranges of 0.1–0.5 s and 0.4–2.0 s for F_a and F_v respectively [66]. These site coefficients are both spectral period and site dependent. Defining the period range is an important part for determination of F_a and F_v values. Many authors [e.g. 13, 67] commented on wider range of period in defining site coefficients by Borcherdt [66]. Various range of F_a and F_v are tested to better match the surface spectra for the corresponding case and site. The range of spectral period that resulted in the best match is 0.01–0.35 s for F_a and 0.35–1.25 s for F_v. In the present study, F_a and F_v have been calculated for period range 0.01–0.35 s and 0.35–1.25 s respectively. The site factor corresponding to zero period i.e. F_{PGA} is also calculated. The calculated F_a and F_v values are given as Table 2. F_a and F_v calculated in this study are higher than NEHRP. For site class C, for PGA between 0.13 and 0.18 g (i.e. G3), F_a and F_v

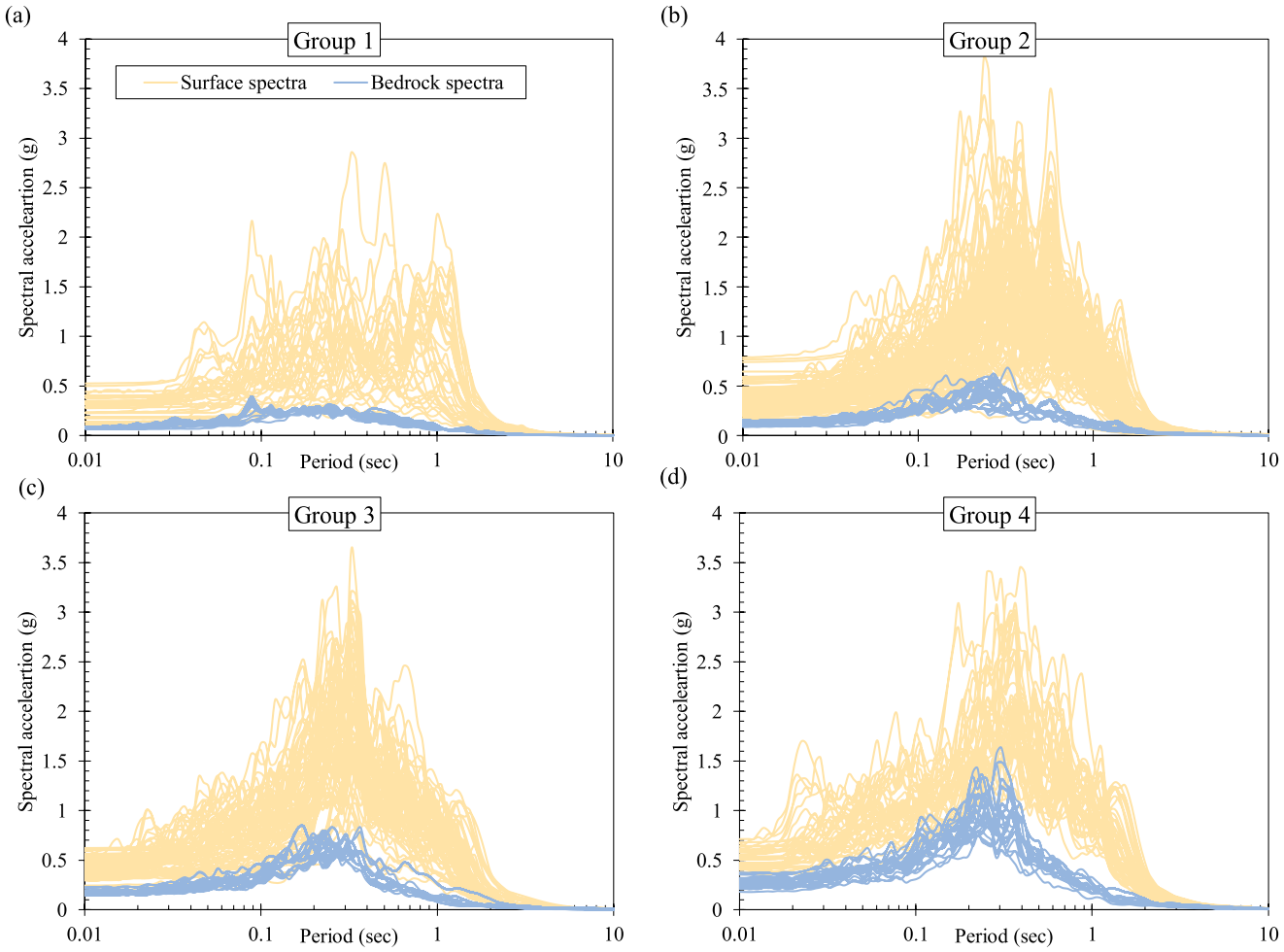

Fig. 10. Comparison of maximum surface spectra with the bedrock spectra for (a) G1, (b) G2, (c) G3, and (d) G4.

calculated in this study is 1.61 and 2.48 respectively, however as per NEHRP estimated F_a and F_v are 1.2 and 1.68 respectively. Further these values are compared with the deep soil site response study carried out by Aboye et al. [13] and Malekmohammadi and Pezeshk [36]. For site class E with V_{S30} equal/less than 180 m/s and PGA between 0.03 and 0.08 g, F_a and F_v values calculated from Aboye et al. [13] are 1.98 and 3.32 which are lower as compared to the present study (See Table 2) Similarly, for site class E, with V_{S30} equal to 180 m/s and PGA between 0.03 and 0.08 g, F_a and F_v values calculated from Malekmohammadi and Pezeshk [36] and present study respectively are 1.592 and 4.390, and 3.063 and 4.159. F_a value calculated in this study has significant variation as compared to the NEHRP, Aboye et al. [13] and Malekmohammadi and Pezeshk [36].

The site factors derived in this study is recommended only for constructing Acceleration design spectra for the Indo Gangetic Basin. The F_{PGA}, F_a and F_v values derived in this study is different from previous study may be due to (1) difference in input layer; (2) region-specific ground motions data; and (3) representative region-specific input parameters. Based on the overall analysis, the major factors that affects the site coefficients are depth of input motion, shear wave velocity of a soil column, G/G_{max} and damping ratio curves.

The site coefficients developed in this study can be used for constructing the acceleration design response spectra for any site in the IGB. The procedure outlines in AASHTO [23] can be summarized in four steps: (1) determine the site class either based on NEHRP; (2) determine PGA at bedrock (PGA_{BR}), SA at 0.2 sec (S_S) and SA at 1.0 sec (S_1) for 10% probability of exceedence in 50 years from probabilistic seismic hazard maps; (3) Based on PGA, S_S and S_1, use the corresponding F_{PGA}, F_a and F_v values to account the site effect; (4) three points of acceleration design response spectra can be derived as

$$PGA = PGA_{BR} \times F_{PGA} \tag{6}$$

$$S_{DS} = F_a S_S \tag{7}$$

$$S_{D1} = F_v S_1 \tag{8}$$

where, S_{DS} and S_{D1} are the design short period (0.2 s) and design long period (1.0 s) spectral response acceleration at ground surface. Fig. 14 shows the typical comparison of the average surface spectra for site class D for all the four groups with the proposed design spectra and NEHRP design spectra. It can be observed from Fig. 14 that for lower PGA value, NEHRP design spectra is predicting less spectral acceleration value as compared to the surface spectra. Similar, observations have been seen for other sites. Fig. 15 shows the comparison of acceleration design response spectra (ADRS) for site class E and site class C constructed using F_{PGA}, F_a and F_v derived in this study. The PGA value used in comparison for group G1, G2, G3 and G4 respectively is 0.07 g, 0.1 g, 0.16 g and 0.23 g. ADRS for site class E and C are compared with the ADRS of soft and medium soil for IS-1893 (2016) respectively. It has

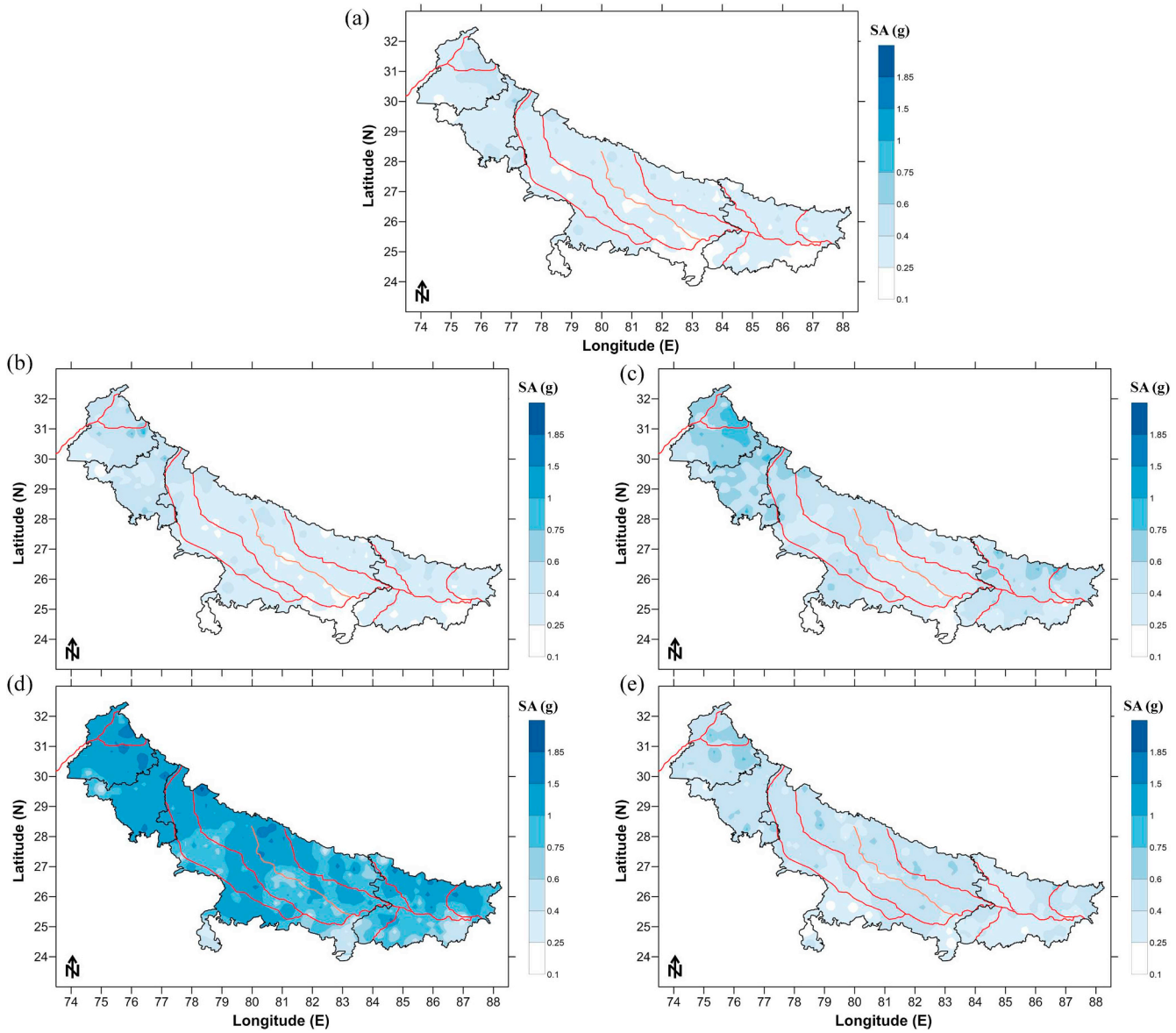

Fig. 11. Distribution of average spectral acceleration (SA) at (a) zero period, (b) 0.02 s, (c) 0.05 s, (d) 0.2 s and (e) 1.0 s at surface for the Indo Gangetic Basin.

been observed that for the same PGA value, ADRS constructed using IS-1893 is underestimating the spectral acceleration values.

8. Conclusion

In the present study, non-linear site response analysis has been carried out for deep profiles in IGB. Firstly, V_S for 275 sites has been determined by carrying out active and passive MASW survey in Punjab, Haryana, Uttar Pradeshand Bihar state in the IGB. Using the non-linear site response analysis, site response parameters at surface have been derived. Further, the spatial variation of surface PGA and SA have been developed for the entire IGB. The bedrock PGA of 0.03–0.24 g increased to 0.1–0.75 g at surface and 0.05–0.35 g at a depth of 150 m. For the deep IGB, high amplification has been observed at depth between 10 and 70 m for few sites near to the Ganga-Yamuna interfluve, Kosi megafan and Sone River due to presence of the low velocity zones. The average SA for most of the IGB at zero period increased from 0.2-0.35 g to 1.0–1.85 g at 0.2 sec and changes to 0.4–0.6 at 1 sec. The maximum surface SA occurs at spectral period between 0.25 and 0.38 sec in this region and it decreased to 0.12–0.15 s at depth of 150 m. For most of the sites, the maximum spectral acceleration has been observed between 0.08 s and 0.5 sec in IGB. The amplification factor in Punjab-Haryana, Uttar Pradesh and Bihar region varies from 2.8 to 3.9, 1.5 to 3.4, 1.8 to 6.3 respectively. The new site factors that are F_{PGA}, $F_a$and F_v, are derived for the IGB for different seismic site class as per NEHRP. F_a and F_v have been calculated for period range 0.01–0.35 s and

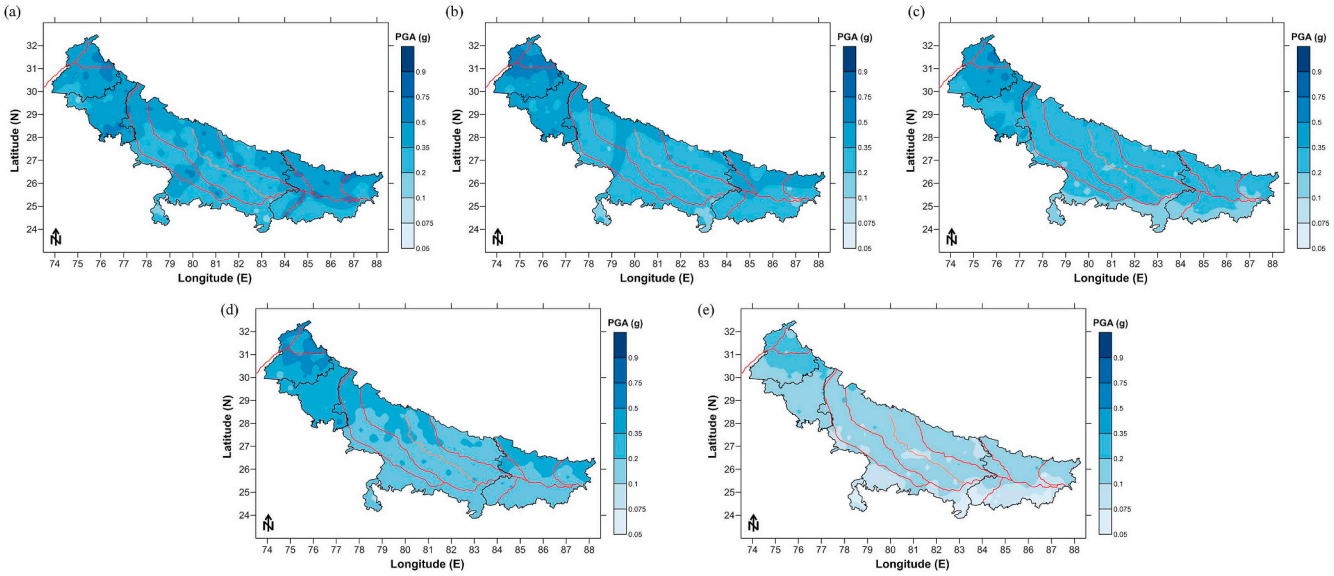

Fig. 12. Distribution of PGA at (a) 10 m, (b) 30 m, (c) 50 m, (d) 100 m, and (e) 150 m depth.

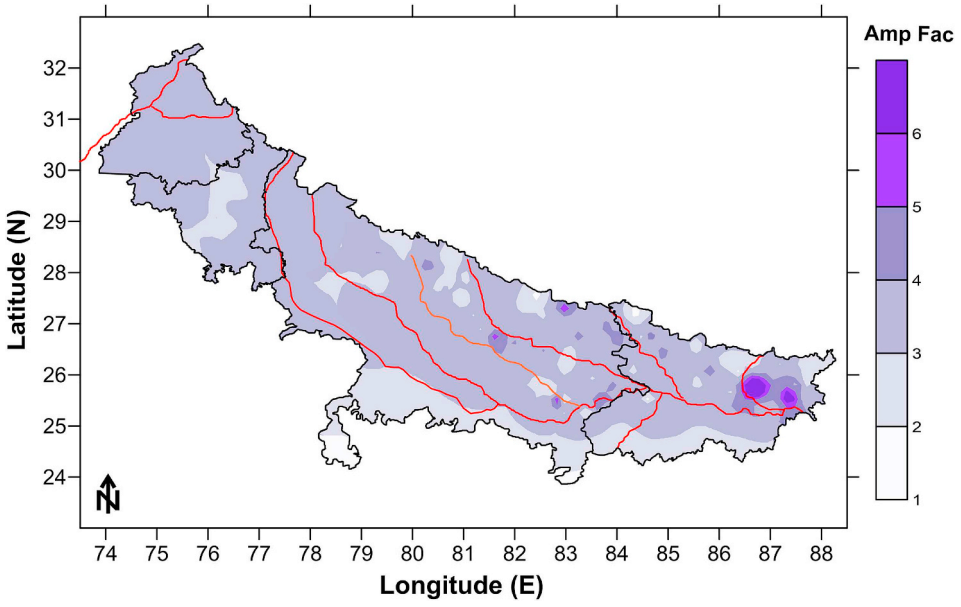

Fig. 13. Spatial variation of amplification factor at surface in case of PGA.

Table 2
Proposed site coefficients for all the four groups with respect to different sites in the IGB.

	Class E			Class D			Class C			Class B		
	F_{PGA}	F_a	F_v	F_{PGA}	F_a	F_v	F_{PGA}	F_a	F_v	F_{PGA}	F_a	F_v
G1	3.013	3.063	4.159	1.869	2.310	3.287	1.422	1.938	2.887	1.015	1.305	1.933
G2	2.710	2.749	3.839	1.680	2.184	2.894	1.354	1.793	2.609	1.013	1.305	1.765
G3	2.595	2.521	3.206	1.572	2.092	3.023	1.314	1.609	2.483	1.010	1.261	1.561
G4	2.321	1.586	2.765	1.362	1.324	2.161	1.290	1.022	1.246	1.001	1.016	1.048

0.35–1.25 s respectively. The newly derived site factors for IGB is more representative than NEHRP as region parameters are used to arrive at results. Considering the newly derived site factors, ADRS for IGB has been derived. It has been further observed that for the same PGA value, ADRS constructed using IS-1893 is underestimating the spectral acceleration values as compared to present study for deep basins. This is the first time such an extensive study has been done for determining the F_{PGA}, F_a and F_v and ADRS for deep sites in the IGB.

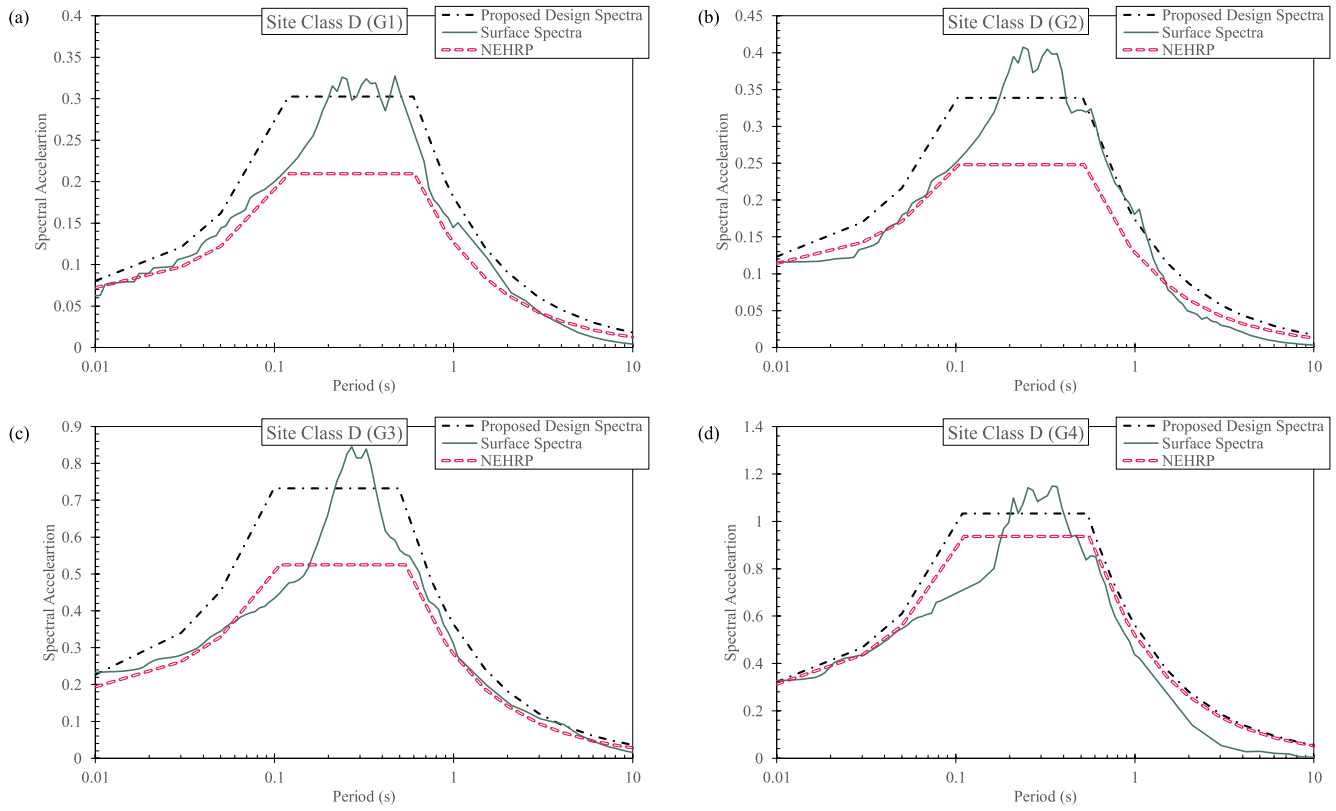

Fig. 14. Typical comparison of surface spectra for site class D for (a) Group 1, (b) Group 2, (c) Group 3, and (d) Group 4 with the proposed design spectra and NEHRP.

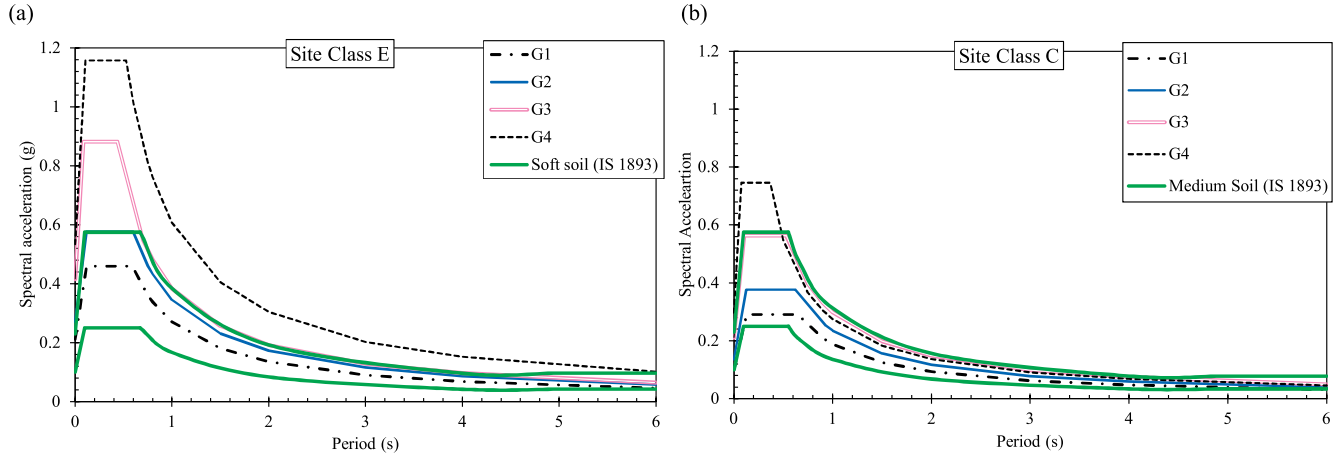

Fig. 15. Typical acceleration response spectrum for (a) Seismic site class E and (b) Site Class C with IS:1893 (2016).

Acknowledgment

The authors thank the Science and Engineering Research Board (SERB) of the Department of Science and Technology (DST), India for funding the project titled “Measurement of shear wave velocity at deep soil sites and site response studies”, Ref: SERB/F/162/2015–2016. Authors also thank the Geological Society of India for providing the Geological and Lithological map required for the study. The Authors would like to thank the PESMOS and ISGN for providing the recorded ground motions.

Appendix A. Supplementary data

Supplementary data to this article can be found online at https://doi.org/10.1016/j.soildyn.2019.105855.

References

[1] Hough S, Bilham R. Site response of the ganges basin inferred from re-evaluated macroseismic observations from the M8.1 shillong 1897, M7.8 Kangra 1905 and 1934 Nepal M8.1 earthquakes. J Earth Syst Sci 2008;117:773–82.
[2] Schiffman C, Bali BS, Szeliga W, Bilham R. Seismic slip deficit in the Kashmir Himalaya from GPS observations. Geophys Res Lett 2013;40:5642–5.
[3] Vernant P, Bilham R, Szeliga W, Drupka D, Skalita S, Bhattacharyya A, Gaur VK. Clockwise rotation of the brahmaputra valley: tectonic convergence in the eastern Himalaya, naga hills and shillong plateau. J Geophys Res 2014;119(8):6558–71.
[4] Ambraseys. Reappraisal of north-Indian earthquakes at the turn of the 20th century. Curr Sci 2000;79:101–6.
[5] Srinagesh D, Singh SK, Chadha RK, Paul A, Suresh G, Ordaz M, Dattatrayam RS. Amplification of seismic waves in the central Indo-Gangetic basin, India. Bull Seismol Soc Am 2011;101:2231–42.
[6] Anbazhagan P, Kumar A, Sitharam TG. Site response of Deep soil sites in Indo Gangetic plain for different historic earthquakes. Proceedings of the 5th international conference on recent advances in geotechnical earthquake engineering and soil dynamics. 2010. p. 12. San Diego, California.

[7] Philips WS, Aki K. Site amplification of coda waves from local earthquakes in central California. Bull Seismol Soc Am 1986;79:627–48.
[8] Wills CJ, Silva W. Shear wave velocity characteristics of Geological units in California. Earthq Spectra 1998;14(3):533–66.
[9] Stewart JP, Liu AH, Choi Y. Amplification factors for spectral acceleration in tectonically active regions. Bull Seismol Soc Am 2003;93:332–52.
[10] Topal T, Doyuran V, Karahanoglu N, Toprak V, Suzen ML, Yesilnacar E. Microzonation for earthquake hazards: yenisehir settlement, Bursa, Turkey. Eng Geol 2003;70(1):93–108.
[11] Pitilakis K. Site effects, recent advances in earthquake geotechnical engineering and microzonation. Geotech Geol Earthq 2004;1:139–97.
[12] Hashash YMA, Tsai CC, Phillips C, Park D. Soil-column depth-dependent seismic site coefficients and hazard maps for the upper Mississippi Embayment. Bull Seismol Soc Am 2008;98:2004–21.
[13] Aboye SA, Andrus RD, Ravichandran N, Bhuiyan AH, Harman N. Seismic site factors and design response spectra based on conditions in Charleston, South Carolina. Earthq Spectra 2015;31(2):723–44.
[14] Kamal Mundepi AK. Site response studies in Dehradun: first step towards microzonation. Natural hazards, spl vol IGC, proceedings of Indian geological congress. 2007. p. 175–81.
[15] Boominathan A, Dodagoudar GR, Suganthi A, Maheshwari RU. Seismic hazard assessment of Chennai city considering local site effects. J Earth Syst Sci 2008;117(S2):853–63.
[16] Anbazhagan P, Sitharam TG. Site characterization and site response studies using shear wave velocity. J Seism Earthq Eng 2008;10(2):53–67.
[17] Naik N, Choudhury D. Site specific ground response analysis for typical sites in Panjim city, Goa. Proceedings of Indian geotechnical conference. 2013. Roorkee, India.
[18] Kumar A, Anbazhagan P, Sitharam TG. Site specific ground response study of deep Indo-Gangetic Basin Using representative regional ground motions, Geo-Congress, State of art and practice in Geotechnical Engineering. 2012. Oakland California, paper no. 1065.
[19] Kumar A, Baro O, Harinarayan N. Obtaining the surface PGA from site response analyses based on globally recorded ground motions and matching with the codal values. Nat Hazards 2016;81:543https://doi.org/10.1007/s11069-015-2095-x.
[20] Building Seismic Safety Council (BSSC). NEHRP recommended provisions for seismic regulations for new buildings and other structures—Part 1: provisions, FEMA- 368; Part 2: commentary, FEMA-369. Washington D.C: Federal Emergency Management Agency; 2003.
[21] American Society of Civil Engineers (ASCE). Minimum design loads for buildings and other structures. Reston, VA: ASCE Standard 7–10; 2010. p. 650.
[22] International Code Council (ICC). International building Code (IBC). VA: Falls Church; 2012. p. 328.
[23] American Association of State Highway and Transportation Officials (AASHTO). LRFD bridge design specifications. second ed. 2011. p. 286. Washington, D.C.
[24] Sastri VV, Bhandari LL, Raju ATR, Dutta AK. Tectonic framework and subsurface stratigraphy of the Ganga Basin. J Geol Soc India 1971;12:222–33.
[25] Rao MBR. The subsurface geology of the indo-gangetic plains. Geol Soc India 1973;14:217–42.
[26] Lyon-Caen H, Molnar P. Gravity anomalies, flexure of the Indian Plate, and the structure, support and evolution of the Himalaya and Ganga Basin. Tectonics 1985;4:513–38.
[27] Srinivas D, Srinagesh D, Chadha RK, Kumar MR. Sedimentary thickness variations in the Indo-Gangetic Foredeep from inversion of receiver functions. Bull Seismol Soc Am 2012;102:2257–65.
[28] Singh IB. Geological evolution of Ganga plain – an overview. J Paleontol Soc India 1996;41:99–137.
[29] Kumar S, Parkash B, Manchanda ML, Singhvi AK. Holocene landform and soil evolution of the western Gangetic Plains: implications of neotectonics and climate. Z Geomorphol 1996;103:283–312. N.F. Suppl.-Bd.
[30] Pati P, Pradhan RM, Dash C, et al. Terminal fans and the Ganga plain tectonism: a study of neotectonism and segmentation episodes of the Indo-Gangetic foreland basin, India. Earth Sci Rev 2015;148:134–49.
[31] Mahajan AK, Virdi KS. Macroseismic field generated by 29 march, 1999 Chamoli earthquake and its seismotectonics. J Asian Earth Sci 2001;19(4):507–16.
[32] Park C, Miller R. Roadside passive multichannel analysis of surface waves (MASW). J Environ Eng Geophys 2008;13:1–11.
[33] Park C, Miller R, Xia J. Imaging dispersion curves of surface waves on multi-channel record. Society of Exploration Geophysicists Expanded Abstracts; 1998. p. 1377–80.
[34] Xia J, Miller RD, Park CB. Estimation of near-surface shear-wave velocity by inversion of Rayleigh waves. Geophysics 1999;64:691–700.
[35] Bajaj K, Anbazhagan P. Seismic site classification and correlation between Vs and SPT-N for deep soil sites in Indo-Gangetic Basin. J Appl Geophys 2019;163:55–72.
[36] Malekmohammadi M, Pezeshk S. Ground motion site amplification factors for sites located within the Mississippi embayment with consideration of deep soil deposits. Earthq Spectra 2015;31(2):699–722.
[37] Electric Power Research Institute (EPRI). Guidelines for Site specific ground motions. Palo Alto, California: November, TR-102293; 1993.
[38] Zhang J, Andrus R, Juang CH. Normalized shear modulus and material damping ratio relationships. J Geotech Geoenviron Eng ASCE 2005;131:453–64.
[39] Anbazhagan P, Prabhakaran A, Madhura H, et al. Nat Hazards 2017;88:1741https://doi.org/10.1007/s11069-017-2944-x.
[40] Bajaj K, Anbazhagan P. Identification of shear modulus reduction and damping curve for deep and shallow sites: kik-net data. J Earthquake Eng 2019https://doi.org/10.1080/13632469.2019.1643807.
[41] Menq FY. Dynamic properties of sandy and gravelly soils. Austin, TX: Ph.D. thesis, Department of Civil Engineering, University of Texas; 2003.
[42] Darendeli MB. Development of a new family of normalized modulus reduction and material damping curves. Austin, Texas: Ph.D. dissertation, University of Texas at Austin; 2001.
[43] Kaklamanos J, Baise LG, Thompson EM, Dorfmann L. Comparison of 1D linear, equivalent-linear, and nonlinear site response models at six KiK-net validation sites. Soil Dyn Earthq Eng 2015;69:207–19.
[44] Anbazhagan P, Uday A, Moustafa SR, Al-Arifi SN. Correlation of densities with shear wave velocities and SPT N values. J Geophys Eng 2016;13:320.
[45] Barani S, Ferrari RD, Ferretti G. Influence of soil modeling uncertainties on site response. Earthq Spectra 2013;29(3):705–32.
[46] Hashash YMA, Kottke AR, Stewart JP, Campbell KW, Kim B, Moss C, Nikolaou S, Rathje EM, Silva WJ. Reference rock site condition for central and eastern North America. Bull Seismol Soc Am 2014;104:684–701.
[47] Silva WJ, Li S, Darragh RB, Gregor N. Surface geology based strong motion amplification factors for the san francisco bay and los angeles areas, prepared for PG&E PEER–task 5.B. Berkeley, CA: Pacific Earthquake Engineering Research Center; 2000.
[48] Kwok AO, Stewart JP. Evaluation of the effectiveness of theoretical 1-D amplification factors for earthquake ground-motion prediction. Bull Seismol Soc Am 2006;96:1422–36.
[49] Govindraju L, Bhattacharya S. Site Response studies for Seismic hazard analysis for Kolkata city. Proceedings of 12th international conference of international association for computer methods and advances in geomechanics. 2008. p. 2899–907.
[50] Anbazhagan P, Sheikh MN, Parihar Aditya. Influence of rock depth on seismic site classification for shallow bedrock regions. 2013https://doi.org/10.1061/(ASCE)NH.1527-6996.0000088.
[51] Ghofrani H, Atkinson GM, Goda K. Implications of the 2011 M9.0 Tohoku Japan earthquake for the treatment of site-effects in large earthquakes. Bull Earthq Eng 2013;11:171–203.
[52] Stewart JP, Chiou SJ, Bray JD, Graves RW, Somerville PG, Abrahamson NA. Ground motion evaluation procedures for performance-based design. Soil Dyn Earthq Eng 2002;2(9–12):765–72.
[53] Baker JW, Cornell CA. Spectral shape, epsilon and record selection. Earthq Eng Struct Dyn 2006;35(9):1077–95.
[54] Baker JW, Lin T, Shahi SK, Jayaram N. New ground motion selection procedures and selected motions for the PEER transportation research program, PEER rep. No 2011/xx. Berkeley: Pacific Earthquake Engineering Research Centre, College of Engineering, University of California; 2011.
[55] Ansal A, Tonuk G. Source and site factors in microzonation. Pitilakis KD, editor. Earthq geotech eng, vols. 73–92. 2007.
[56] Anbazhagan P, Srilakshmi KN, Ketan Bajaj, Sayed SR Moustafa, Nassir S.N. Al-Arifi. Determination of Seismic site classification of seismic recording stations in the Himalayan region using HVSR method. Soil Dyn Earthq Eng. 116, 304-316.
[57] BIS 1893 (Part 1). Indian standard criteria for earthquake resistant design of structures. New Delhi: Bureau of Indian Standards; 2016. Sixth Revision.
[58] Bajaj K, Anbazhagan P. Detailed seismic hazard, disaggregation and sensitivity analysis for Indo Gangetic basin. Pure Appl Geophys 2018. [First Review Completed)].
[59] Motazedian D, Atkinson GM. Stochastic finite-fault modeling based on a dynamic corner frequency. Bull Seismol Soc Am 2005;95:995–1010.
[60] Boore DM. Comparing stochastic point-source and finite-source ground motion simulations: SMSIM and EXSIM. Bull Seismol Soc Am 2009;99:3202–16.
[61] Hashash YMA, Park D. Non-linear one-dimensional seismic ground motion propagation in the Mississippi embayment. Eng Geol 2001;62(1–3):185–206.
[62] Hashash YMA, Musgrove MI, Harmon JA, et al. DEEPSOIL 7.0.5, user manual. Urbana: Board of Trustees of University of Illinois at Urbana-Champaign; 2017.
[63] Schnabel PB, Lysmer J, Seed HB. SHAKE: a computer program for earthquake response analysis of horizontally layered sites, Report EERC 72-12. Berkeley: University of California; 1972.
[64] Sharma ML, Wason HR. Estimation of Seismic Hazard and Seismic zonation at bedrock level at Delhi region. Proceedings of 13th world conference of earthquake engineering, Vancouver, Canada. 2004. paper no 2046.
[65] Phanikanth VS, Choudhury D, Reddy GR. Equivalent-linear seismic ground response analysis of some typical sites in Mumbai. Geotech Geol Eng 2011;29(6):1109–26.
[66] Borcherdt RD. Estimates of site-dependent response spectra for design (methodology and justification). Earthq Spectra 1994;10:617–53.
[67] Park D, Dong K, Chang-Gyun J, Taehyo P. Development of probabilistic seismic site coefficients of Korea. Soil Dyn Earthq Eng 2012;43:247–60.